# Giant Isotropic Nernst Effect in an Anisotropic Kondo Semimetal

Ulrike Stockert,[1] Peijie Sun,[1,†] Niels Oeschler,[1] Frank Steglich,[1] Toshiro Takabatake,[2] Piers Coleman,[3,4] and Silke Paschen[5,*]

[1]*Max Planck Institute for Chemical Physics of Solids, 01187 Dresden, Germany*
[2]*Graduate School of Advanced Sciences of Matter, Hiroshima University, Higashi-Hiroshima 739-8530, Japan*
[3]*Center for Materials Theory, Rutgers University, Piscataway, New Jersey 08855, USA*
[4]*Department of Physics, Royal Holloway, University of London, Egham, Surrey TW20 0EX, United Kingdom*
[5]*Institute of Solid State Physics, Vienna University of Technology, Wiedner Hauptstr. 8-10, 1040 Vienna, Austria*

(Received 3 March 2016; revised manuscript received 29 April 2016; published 14 November 2016)

The "failed Kondo insulator" CeNiSn has long been suspected to be a nodal metal, with a node in the hybridization matrix elements. Here we carry out a series of Nernst effect experiments to delineate whether the severely anisotropic magnetotransport coefficients do indeed derive from a nodal metal or can simply be explained by a highly anisotropic Fermi surface. Our experiments reveal that despite an almost twentyfold anisotropy in the Hall conductivity, the large Nernst signal is isotropic. Taken in conjunction with the magnetotransport anisotropy, these results provide strong support for an isotropic Fermi surface with a large anisotropy in quasiparticle mass derived from a nodal hybridization.

DOI: 10.1103/PhysRevLett.117.216401

There is a wide and growing interest in electron materials with topologically protected excitation spectra, including $Z_2$ topological insulators and topological superconductors [1–3] and, most recently, topologically protected Weyl semimetals [4,5]. Rare-earth heavy-fermion systems have recently emerged as a new venue to explore the interplay of strong correlations with topology [6–9]: the strong electron-electron interactions and spin-orbit coupling make these systems ideal candidates for research in this area. The class of Kondo insulators, such as $SmB_6$, has received much attention as candidate strongly interacting $Z_2$ topological insulators. The little-known family of Kondo semimetals [10–13] may provide a second example of such topological protection. These compounds are considered to be failed Kondo insulators, in which the hybridization gap contains a node that closes the gap in certain directions, giving rise to a semimetal with a pseudogap. Transport studies on these materials have confirmed the presence of a large anisotropy in the magnetotransport, but such anisotropies are not in themselves an indication of a nodal hybridization, and could derive from anisotropic Fermi surface geometries.

In this Letter we carry out a series of magnetothermoelectric measurements on the Kondo semimetal CeNiSn. They reveal that unlike the Hall conductivity, which is highly anisotropic, the large Nernst effect is essentially isotropic. We show how this unexpected isotropy rules out an anisotropic Fermi surface geometry and is a natural consequence of cancellations between mean free path and mass anisotropies expected in a nodal semimetal. This definite understanding of the material's bulk properties is an important prelude to any future studies of putative surface contributions.

CeNiSn is a heavy electron material with emergent semimetallic properties. When it develops coherence at low temperatures, a pseudogap opens in its electronic density of states, as revealed by both tunneling [14,15] and nuclear magnetic resonance [16,17] studies. Modest magnetic fields are sufficient to remove the pseudogap [15]. The material exhibits marked anisotropy in its magnetotransport properties [18–21]. To account for this unusual behavior, Ikeda and Miyake proposed a hybridization model for this Kondo lattice system [10], treating it as a Kondo insulator in which the hybridization gap contains a node along the crystallographic $a$ axis. The presence of this node leads to a V-shaped electronic density of states, a feature that is consistent with both tunneling and NMR measurements [14–17].

An important aspect of this problem which has not received much attention is the Fermi surface and momentum space structure of CeNiSn. One of the most striking features of CeNiSn is the anisotropy in the Hall conductivity. As will be shown below (Fig. 3), it is almost twentyfold between orbits within the basal ($bc$-)plane and those that are perpendicular to it. Conventionally, Hall conductivity anisotropies are associated with corresponding anisotropies in the mean free path: according to the Ong formula, the Hall conductivity is given by [22]

$$\sigma_{xy} = \frac{2e^2}{h}\frac{B_z}{\Phi_0}\int \frac{dk_z}{2\pi} A_l(k_z) \tag{1}$$

where

$$A_l(k_z) = \vec{z}\cdot\oint \frac{\vec{l}\times d\vec{l}}{2} \tag{2}$$

is the area swept out by the mean free path vector

 

$$\vec{l}(\vec{k}) = \vec{v}_{\mathbf{k}}\tau_{\mathbf{k}} = \frac{1}{\hbar}\vec{\nabla}_{\mathbf{k}}E_{\mathbf{k}}\tau_{\mathbf{k}} \quad (3)$$

as $\vec{k}$ moves around the Fermi surface on orbits perpendicular to the applied magnetic field $\vec{B} = (0, 0, B_z)$. $\vec{z}$ is the unit vector along $z$ and $\Phi_0 = h/e$ is the flux quantum.

A twentyfold anisotropy in the Hall conductivity thus requires a corresponding anisotropy in the electronic mean free paths. Although this large anisotropy has been interpreted in terms of the nodal hybridization model, *a priori* the most natural interpretation would be a one-band model with a severely anisotropic Fermi surface. Only in combination with the isotropic Nernst effect presented here we can eliminate this possibility, and provide a definitive interpretation in terms of a nodal Kondo semimetal.

High-quality single crystals (Supplemental Material [23]) grown by the Czochralski technique in a radio-frequency furnace and purified by solid state electron transport [25] were investigated by a steady-state heat transport technique with one heater and differential thermocouples. To conform to the standard $x$, $y$, $z$ notation, in the following we refer to the $a$ axis as $z$, and to $b$ and $c$ as $x$ and $y$, respectively. To measure the Nernst signal $N_{yx} = E_y/\vec{\nabla}_x T$ and the Nernst coefficient $\nu_{yx} = N_{yx}/(\mu_0 H_z)$ we apply a temperature gradient $\vec{\nabla}_x T$ along $x$ and a magnetic field $\mu_0 H_z$ along $z$, which generates an electrical field $E_y$ along $y$. Other $N_{ij}$ are obtained via cyclic index permutations (Supplemental Material [23]). The transverse temperature gradient $\vec{\nabla}_y T$ due to the Righi-Leduc effect was estimated to be less than 2% of the longitudinal gradient $\vec{\nabla}_x T$, making any thermopower contributions to the large Nernst signal negligible. Thus, the experimentally realized adiabatic condition with thermally floating side edges of the sample corresponds, for our samples, approximately to the isothermal condition that is preferentially treated by theories. In addition, measurements of the electrical resistivity and the Hall coefficient (Supplemental Material [23]) were performed in a commercial physical property measurement system (Fig. 1).

Figure 2 shows the temperature dependence of $N_{ij}$ and $\nu_{ij}$ (insets) for three different configurations in different magnetic fields. The absolute values of $N_{ij}$ (and $\nu_{ij}$) strongly increase below 10 K as the pseudogap opens. The maximum value of 120 $\mu$V/K reached for $|N_{yx}|$ at 7 T and 1.8 K is by a factor of 1.2, 4, 5.8, and 130 larger than in the previously studied $f$-electron based "giant" Nernst effect compounds $PrFe_4P_{12}$ [29], $URu_2Si_2$ [30], $SmB_6$ [31], and $CeCoIn_5$ [32], respectively. Interestingly, even larger Nernst signals can arise in simple dilute metals with highly mobile carriers [33].

At small magnetic fields $B < 3$ T the Nernst coefficient of CeNiSn is essentially field independent for all directions (insets of Fig. 2). In the following discussion we concentrate on the 1 T data, which are in the linear response regime (Supplemental Material [23]).

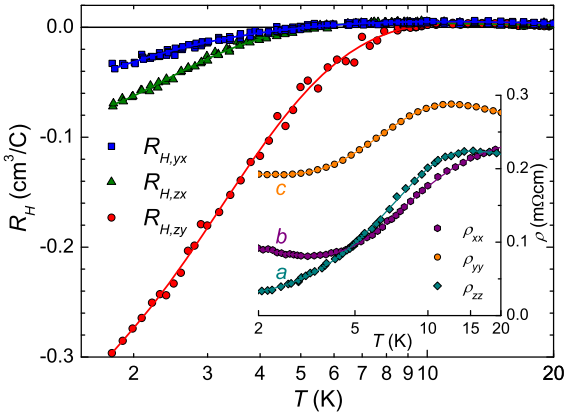


FIG. 1. Temperature dependence of the Hall coefficient $R_H$ and of the electrical resistivity $\rho$ (inset) of CeNiSn for three different configurations and directions. $R_H$ was measured at 1 T, were it is in the linear response regime. The full lines are fits to the data and serve as guides to the eye.

Our most striking observation is that this giant Nernst signal is practically isotropic, in contrast to the highly anisotropic Hall response. It is even more isotropic than the zero-field electrical conductivity $\sigma_{ii}$. This is seen from Fig. 3 where we plot the ratio of the electrical conductivity along the (putative) nodal direction $\sigma_{zz}$ to the arithmetic mean of the conductivities in the plane perpendicular to $z$, $\frac{1}{2}(\sigma_{xx} + \sigma_{yy})$, together with analogous (linear response) Hall and Nernst ratios $\frac{1}{2}(\sigma_{zy} + \sigma_{zx})/\sigma_{yx}$ and $N_{zx}/\frac{1}{2}(N_{yx} + N_{xy})$ (Supplemental Material [23]). At 2 K, the Nernst ratio is of order unity, whereas the conductivity and Hall conductivity ratios reach much larger values of 4 and 18, respectively.

To understand this dichotomy, we now contrast a one-band transport scenario with the nodal hybridization picture. In a one-band picture the severe Hall anisotropy of CeNiSn, $\frac{1}{2}(\sigma_{zy} + \sigma_{zx}) \gg \sigma_{yx}$, would conventionally be understood as a result of Fermi surface curvature. For example, a severely flattened ellipsoidal Fermi surface [Fig. 4(a)] with the dispersion ($\hbar = 1$)

$$E_{\mathbf{k}} = \frac{k_z^2}{2m} + \frac{k_\perp^2}{2m^*} \quad (4)$$

gives rise to a reduction of order $m/m^*$ in the Fermi velocity in the basal plane and, assuming an isotropic scattering rate $\tau_{\mathbf{k}}$, a corresponding reduction of the mean free path and the Hall conductivity in the basal plane. By contrast, in a two-band picture, strong anisotropies of the mean free path can be driven by anisotropies in the hybridization. Suppose $V(\vec{k}) \sim V(k_x \pm ik_y)$ with a node along the $z$ axis [Fig. 4(b)]. The corresponding dispersion is given by

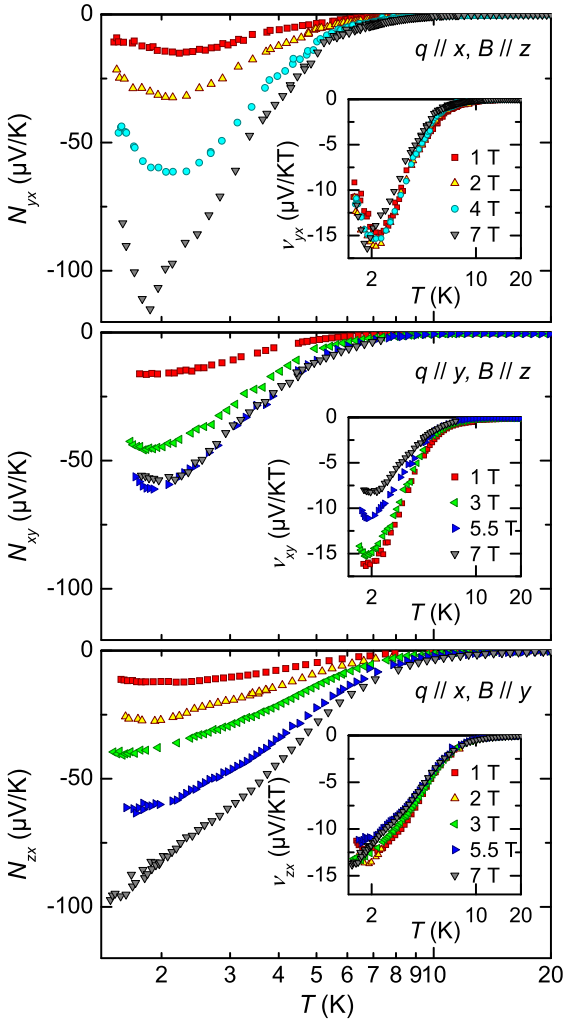


FIG. 2. Temperature dependence of the Nernst signal $N_{ij}$ and Nernst coefficient $\nu_{ij}$ (inset) of CeNiSn for three different configurations, in magnetic fields up to 7 T.

$$E_{\mathbf{k}} = \frac{\epsilon_{\mathbf{k}} + \epsilon_f}{2} \pm \sqrt{\left(\frac{\epsilon_{\mathbf{k}} - \epsilon_f}{2}\right)^2 + V^2 k_\perp^2}. \quad (5)$$

Such hybridized bands are frequently evoked to provide a simple understanding of heavy fermion metals and Kondo insulators [34–37]. Here $\epsilon_{\mathbf{k}} = \vec{k}^2/2m$ is the conduction band dispersion and $\epsilon_f$ is the position of the $f$ level it hybridizes with. In this second scenario, the anisotropy in the quasiparticle velocities does not derive from the Fermi surface curvature, but from the anisotropy in the hybridization, even if the Fermi surface is spherical. Along the $z$ axis, the quasiparticles have the conduction electron dispersion $\epsilon_{\mathbf{k}}$ with the velocity $v_F = k_F/m$, whereas within the basal plane the hybridization with the $f$ state gives rise to a much smaller velocity $v_F^*$, where $v_F^*/v_F \sim V^2 k_F^2/\epsilon_{k_F}^2$ (Supplemental Material [23]). Indeed, Shubnikov–de Haas experiments indicate the presence of very heavy

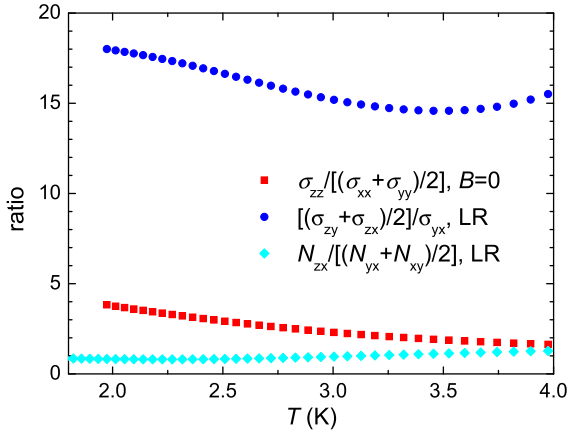


FIG. 3. Ratios of the electrical and Hall conductivity, and the Nernst signal along the putative nodal direction $z$ to the corresponding quantity averaged in the plane perpendicular to $z$ (see legend). Smooth fits to the data (from Fig. 1 for $\sigma_{ii}$ and $\sigma_{ij}$ and from Fig. 2 for $N_{ij}$) were used to calculate the ratios. $\sigma_{ij}$ and $N_{ij}$ were taken in the linear response (LR) regime.

quasiparticles as the field is tilted towards the $z$ axis [21]. Assuming again that $\tau_{\mathbf{k}}$ is isotropic, the velocity (or effective mass) anisotropy then leads to corresponding mean free path and Hall conductivity anisotropies.

Thus, the curvature and hybridization induced mass anisotropies can both give rise to the same Hall anisotropies. We now demonstrate that the anisotropy of the Nernst conductivity $\alpha_{xy}$ distinguishes between the two. According to the Mott formula, $\alpha_{xy}$ is determined by the energy derivative of the Hall conductivity

$$\alpha_{xy} = Q_0 T \left.\frac{\partial \sigma_{xy}}{\partial E}\right|_{E_F} \quad (6)$$

with $Q_0 = (\pi^2 k_B^2/3e)$. Combining this with the Ong formula Eq. (1) we see that the Nernst conductivity is sensitive to the energy dependence of the mean free path around the Fermi surface. In the one-band picture, this anisotropy is entirely determined by the Fermi surface curvature, and thus the Hall and the Nernst signals share the same anisotropy. By contrast, in the hybridization picture, the energy dependence of the mean free path is distinct from the Fermi surface curvature.

To understand this in more detail, it is useful to consider the normalized ratio of the Nernst and Hall conductivities (Nernst-Hall ratio)

$$D_{xy}^* \equiv \left(\frac{\alpha_{xy}}{Q_0 T}\right)\frac{1}{\sigma_{xy}}. \quad (7)$$

Using the Mott formula, Eq. (6), we see that this is the logarithmic energy derivative of the Hall conductivity

$$D^*_{xy} = \left.\frac{\partial \ln \sigma_{xy}}{\partial E}\right|_{E_F}. \quad (8)$$

With the Ong formula, Eq. (1), this results in

$$D^*_{xy} = \left.\frac{\partial \ln}{\partial E}\left(\int dk_z \cdot \vec{z} \cdot \oint \vec{l} \times d\vec{l}\right)\right|_{E_F}, \quad (9)$$

where the integral over $k_z$ is the direction perpendicular to the $xy$ plane. Thus, $D^*_{xy}$ is a measure of those regions of the quasiparticle orbit in which the area swept out by the mean free path is most sensitive to the chemical potential.

In a one-band picture, changing the Fermi energy $E_F$ does not affect the aspect ratios of the Fermi surface. In a simple relaxation time approximation the Fermi momenta, velocities, and mean free paths are all proportional to the square root of the Fermi energy so that, assuming $\tau_{\mathbf{k}}$ to be independent of energy, the logarithmic derivative of the conductivity is given by

$$D^*_{xy} = D^*_{yz} = D^*_{zx} = \frac{3}{2}\frac{1}{E_F}, \quad (10)$$

independent of the direction of measurement. In other words, the anisotropies in densities of states and mean free path compensate one another in all directions and thus the Nernst-Hall ratio is isotropic. A strongly anisotropic Hall conductivity, as observed for CeNiSn, would thus be accompanied by a Nernst conductivity with a qualitatively similar anisotropy, which is at odds with our Nernst measurements on CeNiSn.

However, in the hybridized two-band picture, a change in the Fermi energy produces a very large change in the Fermi momentum of the heavy hybridized band in the plane perpendicular to the nodal axis [Fig. 4(b) right, see Supplemental Material [23] for details], but only a small change in Fermi momentum in the unhybridized direction along the $z$ axis.

In the Supplemental Material [23] we show that in the relaxation time approximation, with an energy independent $\tau_{\mathbf{k}}$, the ratio of Fermi energy $E_F$ to Kondo energy $E_K$ enters in the expression for the Hall conductivity anisotropy but drops out of the corresponding relation for the Nernst conductivity, leading to the Nernst-Hall ratios

$$D^*_{yz} = D^*_{zx} = \frac{1}{E_F} \quad \text{and} \quad D^*_{xy} = \frac{1}{2E_K} \quad (11)$$

and an essentially isotropic Nernst conductivity.

In experiment, it is the Nernst signal $N_{xy}$ rather than the Nernst conductivity $\alpha_{xy}$ that is measured. In this experiment $E_z = \vec{\nabla}_z T = 0$. Using, in addition, $\vec{\nabla} T_y \approx 0$ and $\sigma^2_{xy} \ll \sigma_{xx}\sigma_{yy}$ as estimated to be valid to better than 10% for the data shown in Fig. 3, we obtain

$$\alpha_{yx} \approx \sigma_{yx} N_{xx} + \sigma_{yy} N_{yx}. \quad (12)$$

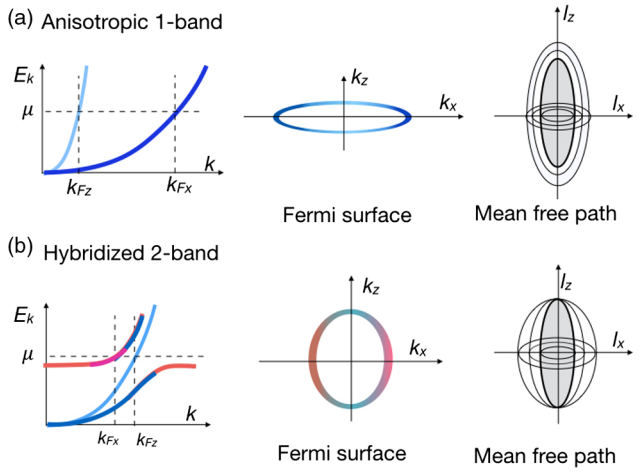


FIG. 4. Contrasting (a) one-band and (b) hybridized two-band models of CeNiSn, showing the dispersion (left), Fermi surface (center), and mean free path as a function of chemical potential (right). In the one-band model, the anisotropy in the mean free path reflects the anisotropy in the effective mass ($m$ along $k_z$ and $m^*$ within the basal plane perpendicular to $k_z$) and thus in the dispersion, but in the two-band model, the anisotropy is driven by nodes in the hybridization along the $z$-axis. Both models give rise to mean free path anisotropy but they differ distinctly in the dependence of this anisotropy on the position of the chemical potential. In the one-band model the mean free path anisotropy is independent of the position of the chemical potential, while in the two-band model, the anisotropy dependence on chemical potential lies predominantly in the basal plane.

For CeNiSn we find that, at 1 T, the first term is negligible below 8 K (Supplemental Material [23]) and thus

$$\alpha_{yx} \approx \sigma_{yy} N_{yx}. \quad (13)$$

In addition, the Nernst ratio is close to 1, in particular below 4 K, where it lies between 0.8 and 1.2. Therefore, the ratio $\alpha_{zx}/\frac{1}{2}(\alpha_{xy} + \alpha_{yx})$ follows the ratio of the electrical conductivities at low temperatures (Fig. 3) and reaches thus values of up to 4. Though less isotropic than the Nernst signal itself, the Nernst conductivities are still much less anisotropic than the Hall conductivities.

The dichotomy between an isotropic Nernst and a strongly anisotropic Hall conductivity provides a valuable signature of nodal hybridization in failed Kondo insulators. One of the unsolved mysteries of Kondo insulators is that all known true Kondo insulators are cubic, whereas the putative nodal Kondo semimetals, including CeNiSn, CeRhSb, and $CeRu_4Sn_4$ [38] develop a conducting pseudogap. In the ongoing search for topological Kondo systems [6,8,9] it is important to understand why the departure from cubic behavior leads, seemingly inevitably, to semimetallic behavior. One interesting possibility is that these systems are related to nodal-line semimetals [39]. An extreme version of nodal semimetallic behavior has also been hypothesized to occur in the quantum critical

semimetal $\beta$-$YbAlB_4$ [40–42]. The Nernst-Hall dichotomy that we have discovered will provide a useful way to confirm nodal behavior in these systems.

In conclusion, we have measured the Nernst coefficient for the Kondo semimetal CeNiSn, showing that the dichotomy between the severely anisotropic Hall conductivity and the giant, yet isotropic Nernst signal can be understood in terms of the nodal hybridization theory of this system. One of the fascinating open questions is whether the semimetallic behavior of CeNiSn is, in any way, topologically protected by the crystal symmetries, as in the case of Weyl semimetals. One of the unexplored and interesting issues of this line of thought is whether CeNiSn might possess novel surface states [43], an aspect that has not been considered in our current analysis. We hope that the Hall-Nernst dichotomy will provide a new impetus for experimental and theoretical work to address these open questions.

We gratefully acknowledge fruitful discussions with K. Behnia and financial support from the Austrian Science Fund Grants No. I623-N16 and No. I2535-N27, the European Research Council Advanced Grant No. 227378, the U.S. Army Research Office Grant No. W911NF-14-1-0497 (S. P.), the National Science Foundation Grant No. DMR 1309929 (P. C.), and the KAKENHI Grants No. JP26400363 and No. JP16H01076 (T. T.). This work was performed in part at the Aspen Center for Physics, which is supported by National Science Foundation Grant No. PHY-1066293.

*Corresponding author.
paschen@ifp.tuwien.ac.at
†Present address: Institute of Physics, Chinese Academy of Sciences, Beijing 100190, China.

[1] L. Fu, C. L. Kane, and E. J. Mele, Phys. Rev. Lett. **98**, 106803 (2007).
[2] J. E. Moore, Nature (London) **464**, 194 (2010).
[3] J. Alicea, Rep. Prog. Phys. **75**, 076501 (2012).
[4] X. Wan, A. M. Turner, A. Vishwanath, and S. Y. Savrasov, Phys. Rev. B **83**, 205101 (2011).
[5] K.-Y. Yang, Y.-M. Lu, and Y. Ran, Phys. Rev. B **84**, 075129 (2011).
[6] M. Dzero, K. Sun, V. Galitski, and P. Coleman, Phys. Rev. Lett. **104**, 106408 (2010).
[7] M. Dzero, J. Xia, V. Galitski, and P. Coleman, Annu. Rev. Condens. Matter Phys. **7**, 249 (2016).
[8] J. D. Denlinger, J. W. Allen, J.-S. Kang, K. Sun, J.-W. Kim, J. Shim, B. I. Min, D.-J. Kim, and Z. Fisk, arXiv:1312.6637.
[9] N. Xu *et al.*, Nat. Commun. **5**, 4566 (2014).
[10] H. Ikeda and K. Miyake, J. Phys. Soc. Jpn. **65**, 1769 (1996).
[11] J. Moreno and P. Coleman, Phys. Rev. Lett. **84**, 342 (2000).
[12] K. I. Nakamura, Y. Kitaoka, K. Asayama, T. Takabatake, G. Nakamoto, H. Tanaka, and H. Fujii, Phys. Rev. B **53**, 6385 (1996).
[13] K. I. Nakamura, Y. Kitaoka, K. Asayama, T. Takabatake, G. Nakamoto, and H. Fujii, Phys. Rev. B **54**, 6062 (1996).
[14] T. Ekino, T. Takabatake, H. Tanaka, and H. Fujii, Phys. Rev. Lett. **75**, 4262 (1995).
[15] D. N. Davydov, S. Kambe, A. G. M. Jansen, P. Wyder, N. Wilson, G. Lapertot, and J. Flouquet, Phys. Rev. B **55**, R7299 (1997).
[16] M. Kyogaku, Y. Kitaoka, H. Nakamura, K. Asayama, T. Takabatake, F. Teshima, and H. Fujii, J. Phys. Soc. Jpn. **59**, 1728 (1990).
[17] K. Nakamura, Y. Kitaoka, K. Asayama, T. Takabatake, H. Tanaka, and H. Fujii, J. Phys. Soc. Jpn. **63**, 433 (1994).
[18] T. Takabatake, G. Nakamoto, M. Sera, K. Kobayashi, H. Fujii, K. Maezawa, I. Oguro, and Y. Matsuda, J. Phys. Soc. Jpn., Suppl. B **65**, 105 (1996).
[19] Y. Inada, H. Azuma, R. Settai, D. Aoki, Y. Ōnuki, T. Takabatake, G. Nakamoto, H. Fujii, and K. Maezawa, J. Phys. Soc. Jpn. **65**, 1158 (1996).
[20] T. Takabatake *et al.*, J. Magn. Magn. Mater. **177–181**, 277 (1998).
[21] T. Terashima, C. Terakura, S. Uji, H. Aoki, Y. Echizen, and T. Takabatake, Phys. Rev. B **66**, 075127 (2002).
[22] N. P. Ong, Phys. Rev. B **43**, 193 (1991).
[23] See Supplemental Material at http://link.aps.org/supplemental/10.1103/PhysRevLett.117.216401 for details on the notations and calculations, which includes Refs. [24–28].
[24] I. Higashi, K. Kobayashi, T. Takabatake, and M. Kasaya, J. Alloys Compd. **193**, 300 (1993).
[25] G. Nakamoto, T. Takabatake, H. Fujii, A. Minami, K. Maezawa, I. Oguro, and A. A. Menovsky, J. Phys. Soc. Jpn. **64**, 4834 (1995).
[26] J. M. Ziman, *Principles of the Theory of Solids* 2nd ed (Cambridge University Press, Cambridge, 1979).
[27] E. H. Sondheimer, Proc. R. Soc. A **193**, 484 (1948).
[28] V. Oganesyan and I. Ussishkin, Phys. Rev. B **70**, 054503 (2004).
[29] A. Pourret, K. Behnia, D. Kikuchi, Y. Aoki, H. Sugawara, and H. Sato, Phys. Rev. Lett. **96**, 176402 (2006).
[30] R. Bel, H. Jin, K. Behnia, J. Flouquet, and P. Lejay, Phys. Rev. B **70**, 220501 (2004).
[31] Y. Luo, H. Chen, J. Dai, Z. A. Xu, and J. D. Thompson, Phys. Rev. B **91**, 075130 (2015).
[32] R. Bel, K. Behnia, Y. Nakajima, K. Izawa, Y. Matsuda, H. Shishido, R. Settai, and Y. Ōnuki, Phys. Rev. Lett. **92**, 217002 (2004).
[33] K. Behnia and H. Aubin, Rep. Prog. Phys. **79**, 046502 (2016).
[34] N. F. Mott, J. Physique Colloque **41**, 51 (1980).
[35] G. Aeppli and Z. Fisk, Comments Cond. Matter. Phys. **16**, 155 (1992).
[36] H. Tsunetsugu, M. Sigrist, and K. Ueda, Rev. Mod. Phys. **69**, 809 (1997).
[37] P. S. Riseborough, Adv. Phys. **49**, 257 (2000).
[38] V. Guritanu *et al.*, Phys. Rev. B **87**, 115129 (2013).
[39] C. Fang, Y. Chen, H.-Y. Kee, and L. Fu, Phys. Rev. B **92**, 081201 (2015).
[40] S. Nakatsuji *et al.*, Nat. Phys. **4**, 603 (2008).
[41] Y. Matsumoto, S. Nakatsuji, K. Kuga, Y. Karaki, N. Horie, Y. Shimura, T. Sakakibara, A. H. Nevidomskyy, and P. Coleman, Science **331**, 316 (2011).
[42] A. Ramires, P. Coleman, A. H. Nevidomskyy, and A. M. Tsvelik, Phys. Rev. Lett. **109**, 176404 (2012).
[43] P. Chang, O. Erten, and P. Coleman, arXiv:1603.03435.